Study on S-shaped region of pump turbine based on Omega vortex analysis method and entropy production theory

Zhenggui Li[1,2*], Hongji Zeng[1,2], Kun Wang[1,2], Xiaodong Peng[1,2], Shengnan Yan[1,2], Qin Zhao[1,2]

(1. *Key Laboratory of Fluid and Power Machinery, Ministry of Education (Xihua University), Chengdu 610039, China*;
2. *Key Laboratory of Fluid Machinery and Engineering of Sichuan Province, Xihua University, Chengdu 610039, China*)

Abstract: In order to comprehensively analyze the operation instability of the pump turbine S-shaped region, this paper uses DDES turbulence model to calculate the model pump turbine from the perspective of the evolution law of runner vortex and draft tube vortex rope and entropy production rate, combined with experiments. The results show that the numerical simulation is in good agreement with the experiment. *Omega* vortex analysis method is more accurate than other vortex recognition methods because it is not affected by the threshold value. The vortices at the runner region under the runaway condition and the turbine brake condition develop towards the vaneless space and the blade pressure surface respectively, which will cause the flow obstruction and blade separation. The overall vorticity of the reverse pump condition is the largest. The vortex rope of the draft tube under runaway and turbine brake conditions is columnar in shape and has very high rotational strength. The vortex rope under reverse pump conditions is prone to fracture and form scattered vortices, impeding the normal movement of the fluid. The entropy production rate of the spanwise surface near the upper ring and the lower crown is greater than the middle spanwise surface due to the boundary layer effect. And the energy dissipation in the runner under reverse pump conditions is characterized by high at both ends of the runner and low in the middle. The energy dissipation near the wall of the straight cone section of the draft tube is large due to the squeezing effect of the vortex rope on the flow.

Keywords: pump turbine, S-shaped region, vortex analysis method, vortex evolution, entropy production rate
DOI: 10.25165/j.ijabe.20231603.7831

Citation: Li Z G, Zeng H J, Wang K, Peng X D, Yan S N, Zhao Q. Study on S-shaped region of pump turbine based on Omega vortex analysis method and entropy production theory. Int J Agric & Biol Eng, 2023; 16(3): 102–109.

1 Introduction

Climate has a critical impact on agricultural production. In view of the current climate problem of global warming, China will strive to achieve carbon peak by 2030 and carbon neutralization by 2060[1]. Pump turbine is a special hydraulic machinery that integrates the two opposite functions of pump and turbine, and S-shaped region is the most unstable area in its power generation condition[2]. When operating in S-shaped region, the fluid in the pump turbine presents strong nonlinear turbulent motion, accompanied by strong vibration of the unit[3].

For the study of S-shaped region, Wang et al.[4] studied the pressure pulsation mechanism under turbine brake conditions and reverse pump conditions, and found that there are high amplitude and low frequency pressure pulsations under these two conditions, which are caused by reflux and vortex in vaneless space respectively. Kinoue et al.[5] studied the start-up process of low specific speed pump turbines and found that the internal flow pattern in S-shaped region was very disordered. Zhang et al.[6] studied the influence of rotor-stator interaction and rotating stall in S-shaped region on pressure pulsation by combining test and simulation. It was found that the pressure pulsation was most affected by the opening of guide vanes under the working condition of hydraulic turbine, and the pressure pulsation of draft tube was mainly due to the combined action of rotating stall and vortex rope. Fu et al.[7] studied the transient process of pump turbine load rejection by using UDF and dynamic grid, and it is proved that pump turbine will produce huge pressure pulsation and a large amount of energy dissipation when running under the runaway conditions.

Because the flow in the fluid machinery is difficult to observe in engineering practice, scholars have been committed to the study of vortex in fluid machinery for a long time. Liu et al.[8] proposed a series of vortex identification methods and defined the third-generation vortex identification method of Liutex system. Krappel et al.[9] adopt the improved IDDES turbulence model to simulate the internal flow of pump turbine, and use the pressure isosurface to identify that the vortex rope in the draft tube is curved. Mao et al.[10] studied the flow characteristics of pump turbine during load rejection, and found that the increase of liquid flow angle is the main reason for the flow instability in the runner channel, and the eddy current in the water ring area is the main reason for preventing the flow from entering the runner region.

Kye et al.[11] found that under LES turbulence model, the rotor-stator interaction between centrifugal pump impeller and volute will produce large vorticity at the tongue. Ji et al.[12] analyzed the vortex structure of reverse pump conditions and found that the existence of the high-speed water retaining ring in the vaneless space makes it difficult for the water flow to pass through the vaneless space. Liu et al.[13] studied the development process of the vortex in the pump turbine through PIV test, and found that the vortex in the vaneless space is closely related to strong pressure pulsation and S

Received date: 2022-08-01 **Accepted date:** 2023-03-29
Biographies: Hongji Zeng, MS candidate, research interest: fluid machinery, Email: 704447856@qq.com; **Kun Wang**, MS candidate, research interest: fluid machinery, Email: 1191515825@qq.com; **Xiaodong Peng**, Professor, research interest: turbine, Email: mypxiaod@126.com; **Shengnan Yan**, Lecture, research interest: turbine, Email: yanshn@mail.xhu.edu.cn; **Qin Zhao**, Professor, research interest: fluid mechanics, Email: zhaoqin7579@163.com
***Corresponding author: Zhenggui Li**, Professor, research interest: fluid machinery. Xihua University, Chengdu 610039, China. Tel: +86-17602832345, Email: lzhgui@mail.xhu.edu.cn

characteristic. However, the flow field analysis cannot study the energy dissipation in the S-shaped region, which requires the introduction of entropy production theory.

Kan et al.[14] proved that the energy loss in the volute area is mainly caused by the strong wall effect near the wall. Fu et al.[15] proved that the hydraulic loss in the process of load rejection of pump turbine is closely related to vortices such as separation vortex and return vortex by combining TEST and CFD. Chen[16] carried out a comprehensive study on the entropy production rate of the flow field of various components in the S-shaped region of pump turbine, and found that the entropy production rate in S-shaped region was higher than that in the normal operation area. It is found that there is still little research on the combination of vortex analysis and entropy production analysis in S-shaped region of pump turbine.

To sum up, based on the improved Omega vortex analysis method and entropy production theory, this paper studies the vortex law and their energy dissipation of the three most typical conditions in S-shaped region: runaway condition, turbine brake condition, and reverse pump condition, and comprehensively analyzes the operation instability of the pump turbine under these three working conditions, so as to provide reference for engineering practice.

2 Calculation method and theory

2.1 Omega vortex analysis method

Vortex motion is a common form of motion in fluid machinery, which will greatly affect the operation safety of pump turbines, and the vortex motion in fluid machinery is often difficult to observe, laying hidden dangers for engineering safety. With the development of CFD, a vortex analysis method was gradually developed which does not depend on the selection of coordinates and rotation changes[17], that is, the motion of the vortex in the pump turbine can be explored by analyzing the results of CFD through the vortex analysis method.

At present, the most common vortex analysis methods are Q-criterion and λ_2-criterion. The Q-criterion uses the second matrix invariant Q of the velocity gradient tensor to identify the vortex. The Q-criterion reflects a balance between the rotation and deformation of a fluid micro-cluster in the flow field. If Q>0, it means that the rotation is greater than the deformation, that is, there is vortex, and Q<0 means that the shear strain dominates the flow. λ_2-criterion is an improvement on the method of searching the region of the minimum pressure, and defines the region where the symmetric tensor $S^2+\Omega^2$ has two negative eigenvalues as a vortex. Due to the symmetry of $S^2+\Omega^2$, its eigenvalue size is sorted $\lambda_1>\lambda_2>\lambda_3$. If $\lambda_2<0$, there are two negative eigenvalues, and the minimum pressure exists, which determines that this region is a vortex. But for a long time, they have been affected by the selection of threshold value, which is difficult to avoid and easy to cause inaccurate results. Therefore, Liu proposed a new *Omega* vortex identification method[18], so that the results are not affected by the threshold selection, which greatly improves the reliability of vortex analysis. Liu decomposes the vorticity into rotating part and non-rotating part, and introduces a new parameter Ω to represent the ratio of rotating part and overall vorticity, as shown in the following formula.

$$\omega = R + S \tag{1}$$

$$\Omega = \frac{\|B\|_F^{\ 2}}{\|A\|_F^2 + \|B\|_F^2} \tag{2}$$

In order to prevent the denominator from being zero when using, add a very small positive number ε to the denominator of the above equation.

$$\Omega = \frac{\|B\|_F^{\ 2}}{\|A\|_F^{\ 2} + \|B\|_F^{\ 2} + \varepsilon} \tag{3}$$

where, ω represents total vorticity; R represents vortical vorticity; S represents non rotating vorticity; B represents antisymmetric tensor; and A represents symmetric tensor.

So theoretically, as long as $0.5<\Omega<1$, the rotation intensity is greater than the shear, that is, there is vortex. For the runner area, the actual experience generally takes $\Omega \in (0.51, 0.60)$ to identify the vortex[19, 20].

2.2 Entropy production theory

The relationship between the entropy production rate and energy dissipation rate is expressed as follows:

$$\dot{S}_D^{\cdots} = \frac{\dot{Q}}{T} \tag{4}$$

where, $\dot{S}_D^{\cdots}$ represents entropy production rate; $\dot{Q}$ represents energy dissipation rate.

Therefore, the entropy production rate can characterize the energy dissipation. When the fluid flow inside the pump turbine is turbulent, the entropy production rate is influenced by the time-averaged and pulsating velocities, expressed as follows:

$$\dot{S}_D^{\cdots} = \dot{S}_{\bar{D}}^{\cdots} + \dot{S}_{\tilde{D}}^{\cdots} \tag{5}$$

$$\dot{S}_{\tilde{D}}^{\cdots} = \frac{\mu_{eff}}{T}\left\{2\left[\left(\frac{\partial u_1'}{\partial x_1}\right)^2 + \left(\frac{\partial u_2'}{\partial x_2}\right)^2 + \left(\frac{\partial u_3'}{\partial x_3}\right)^2\right] + \left(\frac{\partial u_2'}{\partial x_1} + \frac{\partial u_1'}{\partial x_2}\right)^2 + \left(\frac{\partial u_3'}{\partial x_1} + \frac{\partial u_1'}{\partial x_3}\right)^2 + \left(\frac{\partial u_2'}{\partial x_3} + \frac{\partial u_3'}{\partial x_2}\right)^2\right\}^2 \tag{6}$$

$$\dot{S}_{\bar{D}}^{\cdots} = \frac{2\mu}{T}\left[\left(\frac{\partial \bar{u}_1}{\partial x_1}\right)^2 + \left(\frac{\partial \bar{u}_2}{\partial x_2}\right)^2 + \left(\frac{\partial \bar{u}_3}{\partial x_3}\right)^2\right] + \frac{\mu}{T}\left[\left(\frac{\partial \bar{u}_2}{\partial x_1} + \frac{\partial \bar{u}_1}{\partial x_2}\right)^2 + \left(\frac{\partial \bar{u}_3}{\partial x_1} + \frac{\partial \bar{u}_1}{\partial x_3}\right)^2 + \left(\frac{\partial \bar{u}_2}{\partial x_3} + \frac{\partial \bar{u}_3}{\partial x_2}\right)^2\right]^2 \tag{7}$$

$$\mu_{eff} = \mu + \mu_t \tag{8}$$

where, $\dot{S}_{\tilde{D}}^{\cdots}$ is the entropy production rate due to pulsating velocity; $\dot{S}_{\bar{D}}^{\cdots}$ is the entropy production rate due to the time-averaged velocity; μ_{eff} is fluid effective dynamic viscosity; μ_t is turbulent power viscosity.

For the k-ω turbulence model, the entropy production rate of the pulsating velocity can be calculated by the following formula:

$$\dot{S}_{\tilde{D}}^{\cdots} = \beta\frac{\rho\omega k}{T} \tag{9}$$

where, β=0.09, ω is turbulent vortex viscous frequency; k is turbulent kinetic energy.

3 Numerical calculation model

3.1 Computational domain and grid irrelevance verification

In this study, a pump turbine model machine was used for calculations. The overflow components included the volute, stay vanes, guide vanes, runner blades, and draft tube. The geometric parameters of the model are listed in Table 1.

In this study, ICEM software is used to mesh the whole model. Because the structured mesh can easily realize the boundary fitting of the region and is suitable for the calculation of fluid and surface stress concentration, the whole model adopts structured mesh[21,22]. The grid independence is verified by taking the normal operating condition of the hydraulic turbine as the calculation condition point.

Table 1 Parameters of the model

Parameter	Value
Runner inlet diameter D_1/mm	477.5
Runner outlet diameter D_2/mm	240
Number of runner blades Z_1	9
Number of stay vanes Z_2	20
Number of guide vanes Z_3	20

It can be seen from Figure 1 that the head and efficiency are close to the test data when the number of grids is greater than 4.72 million, and tend to be stable. Considering the calculation accuracy, the model with a total number of grids of 7.15 million is finally selected as the grid model for this calculation. The grid division diagram of pump turbine model is shown in Figure 2.

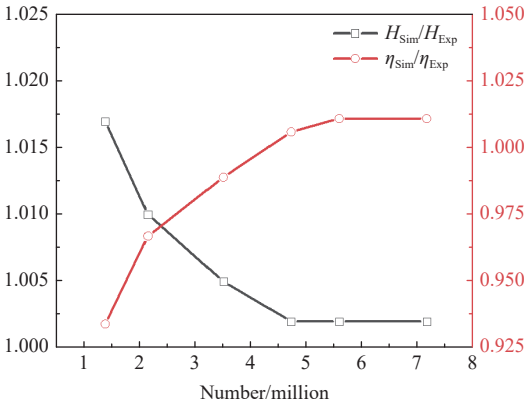

Figure 1 Grid independence verification

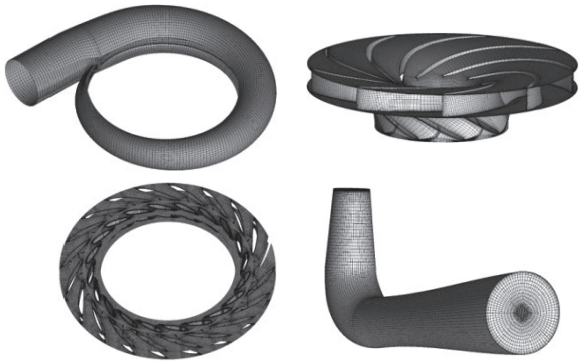

Figure 2 Grids of different parts

3.2 Turbulence model

For a long time, *k*-*ω* model and *k*-*ε* model have been widely used in the study of CFD. Later, Spalart et al.[23] first proposed the Detached-Eddy Simulation (DES), whose core idea is to use Reynolds Average Navier-Stokes (RANS) turbulence model in the near wall region, but Large-Eddy Simulation (LES) model is used in the mainstream region. Spalart et al.[24] later proposed the Delayed Detached-Eddy Simulation (DDES), which introduced a delay function into the Detached-Eddy Simulation and reconstructed the length scale, which largely avoided the MSD problem. Therefore, DDES model can better reflect the vortex dominated flow than the traditional *k*-*ε* model. In this calculation, SST *k*-*ω* model is used for Steady calculation, and DDES model is used for Transient calculation.

3.3 Boundary condition

In this calculation, FLUENT is used for numerical calculation in the full fluid domain. The inlet boundary conditions of the model are set as mass-flow inlet, and the outlet is set as pressure outlet. The flow field is coupled by SIMPLEC method, and the solid wall adopts non slip boundary conditions. The Steady rotation of the runner is set to frame motion, and the Transient rotation is set to mesh motion. Taking the time taken for the runner to rotate by 1° as a time step and the maximum number of iteration steps is 100, all the calculation results of energy characteristics are obtained without considering cavitation.

4 Test verification

The numerical calculation results at different operating points are processed to convert into unit parameters, and the n_{11}-Q_{11} curve is drawn and compared with the n_{11}-Q_{11} curve of the model, as shown in Figure 3. It can be found that the n_{11}-Q_{11} curve shows an anti-S shape. At this time, the same n_{11} may correspond to two or even three Q_{11}, which will make it difficult for the pump turbine to connect to the grid or fail to achieve no-load stability after load shedding, resulting in tripping.

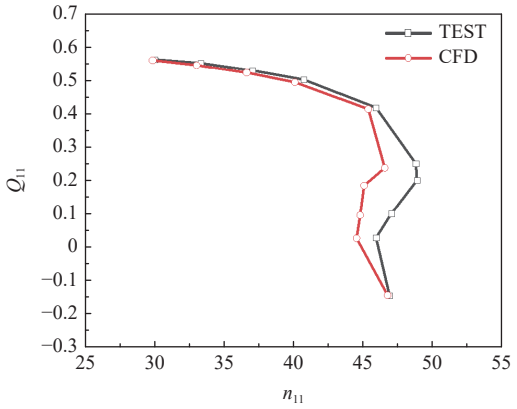

Figure 3 Characteristic curve

At the same time, it can be seen that the tolerance of test and numerical calculation is small, and the maximum tolerance appears near the runaway condition, but it is still less than 7.8%, which is acceptable. Therefore, the three most typical working conditions in S-shaped region: runaway condition, turbine brake condition, and reverse pump condition, are taken for numerical calculation. The specific calculation operating points are listed in Table 2.

Table 2 Calculated working points

Working condition	n_{11}	Q_{11}
Runaway condition,OP1	45.05	0.1855
Turbine brake condition,OP2	44.76	0.0958
Reverse pump condition,OP3	46.75	−0.1444

5 Analysis of vortex and entropy production rate in runner channel of S-shaped region

5.1 Vortex variation law

The discussion of the flow characteristics in the runner region must be inseparable from the analysis of vortices. As mentioned earlier, compared with *Q*-criterion and λ_2-criterion. *Omega* vortex analysis method is not affected by the selection of threshold value, and has higher accuracy for vortex identification. Here, the runaway condition is taken as an example to prove the advantages of *Omega* vortex analysis method. The vortex identification results of the *Q*-criterion, the λ_2-criterion and the *Omega* vortex analysis method for the same operating condition at different thresholds are given in Figure 4.

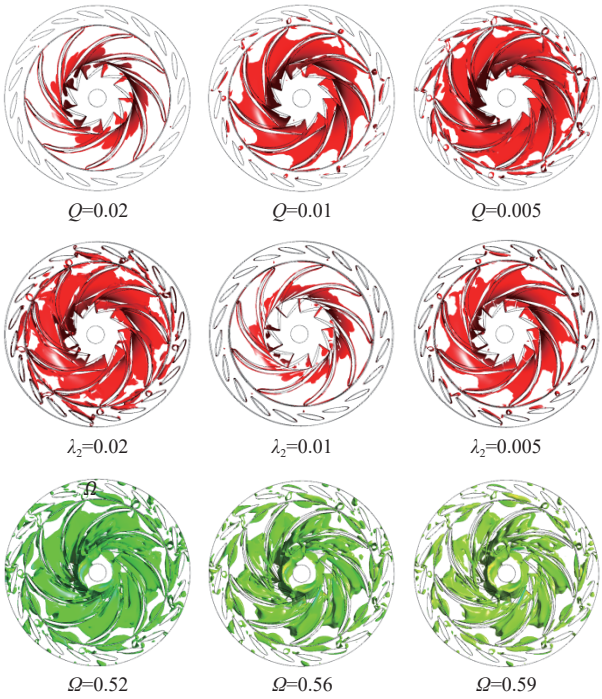

Figure 4 Comparison of different threshold recognition results

As can be seen from Figure 4, the Q-criterion and λ_2-criterion are extremely sensitive to the selection of threshold, and even a small number of vortices can be identified at some scales (such as Q, λ_2=0.02). And there is no unified standard for the threshold selection of Q-criterion and λ_2-criterion, which is easy to cause the result distortion and lack of reliability. In contrast, the threshold change of Omega method only affects some vortices with weak rotation intensity, and strong vortices can be identified under different thresholds.

In order to explore the evolution law of vortices in the S-shaped region of pump turbine under various working conditions, Omega vortex analysis method is used to identify the transient vortices of the runner under three working conditions. At the same time, take Ω=0.59, and the results are shown in Figure 5.

When the pump turbine is in runaway condition, its speed reaches the maximum. It can be seen from Figure 5a that when the pump turbine rotates for 1/3 turn under runaway condition, the vortices are mainly scattered small-scale vortices, which are periodically distributed at the inlet of the runner channel. These vortices caused the blockage of the channel. As the runner rotates to 2/3 turn, the small independent vortices at the runner channel inlet develop into slender large vortices, and the blade suction surface forms a large area of blade passage vortices. After another 120° rotation, it can be clearly seen that the annular vortex is formed in the vaneless space because the high speed of runaway condition and strong rotor-stator interaction have a great impact on the vaneless space. The circulation in the vaneless space will seriously hinder the flow of water and cause abnormal vibration of the pump turbine.

When the torque generated by centrifugal force is greater than the sum of water torque and unit resistance torque, braking torque

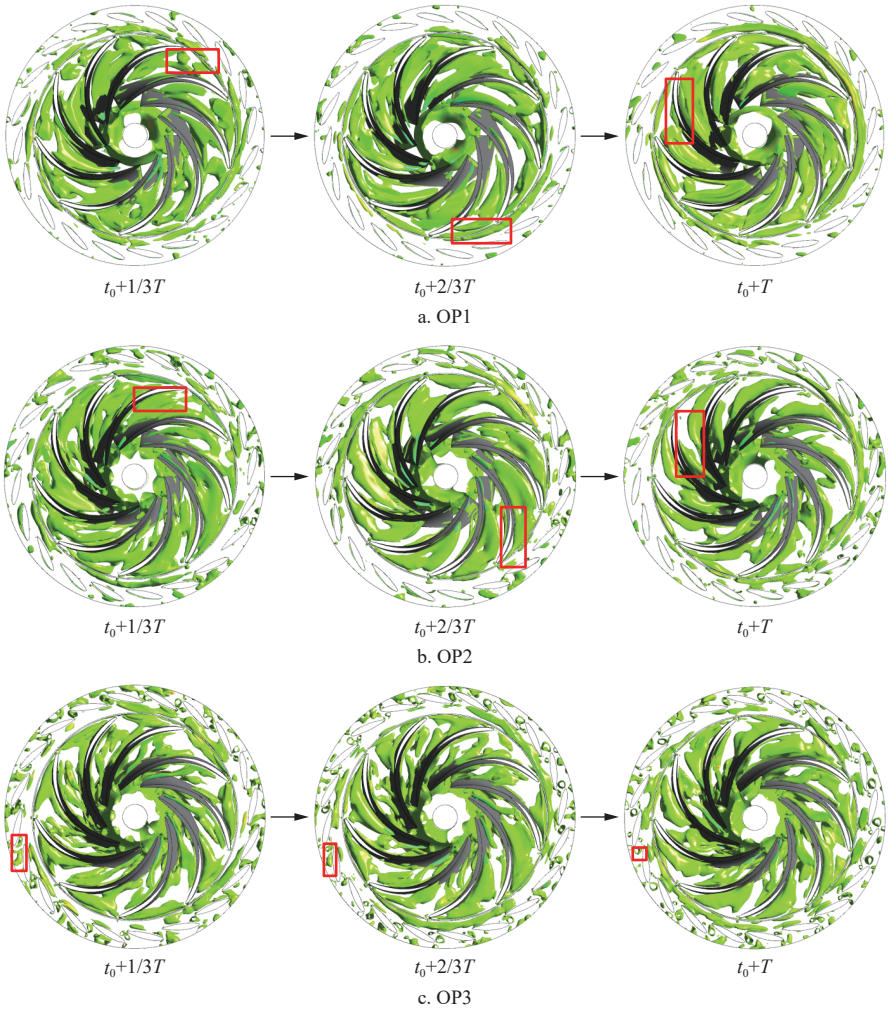

Figure 5 Vortices evolution law

will be generated, and the runner speed will begin to decline, entering the turbine brake condition. Due to the strong periodicity of the vortex distribution, Figure 5b fixedly tracks the vortex in a runner channel. It can be found that under turbine brake conditions, the vortex is initially distributed on both the suction surface and the pressure surface, but gradually converges to the pressure surface with rotation. At this time, the rate of flow is small and the runner speed is high, so the blade wall happens to de-flow, causing flow separation and making the runner channel long and narrow. Finally, there is no vortex structure on the suction surface, and all the vortices are close to the pressure surface, which is also detrimental to the flow stability.

When the water torque is greater than the sum of the centrifugal torque and the resistance torque of the unit, the unit starts to accelerate and enter the reverse pump condition. At this time, the rotation direction of the blade is still the rotation direction of the turbine condition, but the incoming flow direction and the rotation direction do not match, which is easy to cause the water flow to accumulate at the tail of the blade. From Figure 5c, it can be seen that the vortices in the runner flow channel are significantly less than OP1 and OP2, but a large number of vortices in the stagnant flow channel start to appear in the stay-guide vanes, and these vortices formed by the secondary and cross-flow will further obstruct the flow out. And in one rotation, because the flow rate is too small, the vortex scale in stay-guide vanes is also decreasing, and finally each flow channel is distributed with small-scale vortex. Reverse pump conditions can cause severe vibration of the unit, and in engineering practice is a condition zone that must be avoided.

5.2 Comparison of maximum vorticity

The evolution and separation of vortices in each condition are discussed in the previous paper by Omega vortex analysis method. *Omega* vortex analysis method is defined based on the ratio of vortical vorticity to overall vorticity, and the vorticity comes from the velocity gradient of the flow field[25], which is an intuitive embodiment of flow stability[26]. Therefore, this paper quantitatively analyzes the maximum vorticity in the main flow area under various conditions, as shown in Figure 6.

It can be seen from Figure 6 that the vorticity of the stay-guide vanes under the three working conditions is much smaller than that of the runner region and the vaneless space. The vorticity in the vaneless space is the largest under runaway conditions and turbine brake conditions, and the rotor-stator interaction has a great impact on the flow. Because the blade speed is high and the flow is small, there will be obvious flow separation in the runner region under these two working conditions, so there will also be a large velocity gradient. Under the reverse pump condition, because the rotation direction of the runner does not match the direction of incoming flow, it will be difficult for the fluid to flow out of the runner region. At this time, the maximum vorticity in the runner region is the largest under the three working conditions, reaching 206 610 s^{-1}, and the maximum vorticity in the vaneless space under the reverse pump condition also has 174 941 s^{-1}, which further proves that the reverse pump condition is the working condition that should be avoided as far as possible in the engineering practice.

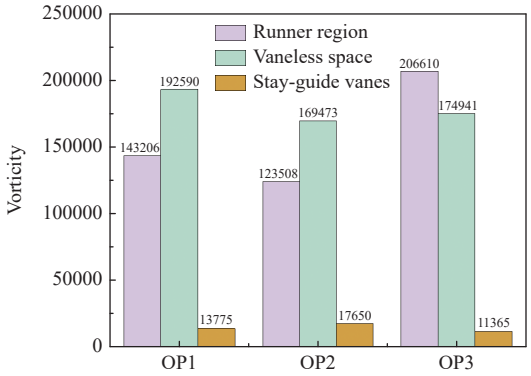

Figure 6 Comparison of maximum vorticity

5.3 Entropy production rate distribution of runner channel

The entropy production theory that has emerged in recent years allows scholars to analyze the S-shaped region in conjunction with energy dissipation. Therefore, this paper studies the distribution of entropy production rate under three conditions and obtains the entropy production rate of different spanwise surfaces of runner channel in Figure 7. Meanwhile, the average entropy production rate of different spanwise surfaces was quantified and compared, as shown in Figure 8. Sp0.1 is the spanwise surface close to the upper crown, Sp0.5 is the middle spanwise surface, Sp0.9 is the spanwise surface close to the lower ring, and the inflow direction is the left side of Figure 7 (runaway condition, turbine brake condition is the stay-guide vanes direction, reverse pump condition is the draft tube direction). The energy dissipation rate is characterized by the entropy production rate.

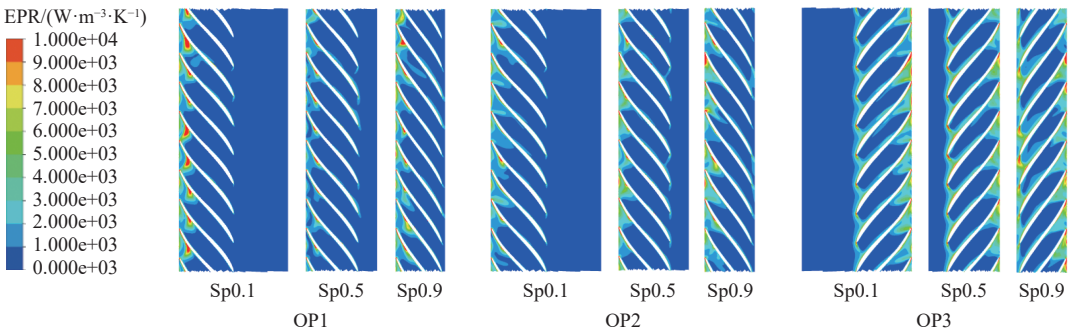

Figure 7 Entropy production rate of different spanwise surfaces in runner channel

It can be seen from Figure 7 that the entropy production rate of the three working conditions is distributed periodically. Under the runaway condition, the energy loss is mainly concentrated on the pressure surface at the head of runner blades, and the entropy production rate is the largest on the Sp0.1 spanwise surface. This is because the high runner speed of runaway condition will form a large velocity gradient at the runner channel inlet, the kinetic energy dissipation is serious, and the blade pressure surface is greatly affected by the direct impact of incoming flow, so a lot of mechanical energy dissipation will be caused here. The entropy

production rate in the middle of the runner channel is significantly reduced. When the pump turbine is under turbine brake condition, flow separation and rotor-stator interaction lead to not only high entropy production rate on the blade pressure surface, but also significantly increased energy dissipation at the runner channel inlet.

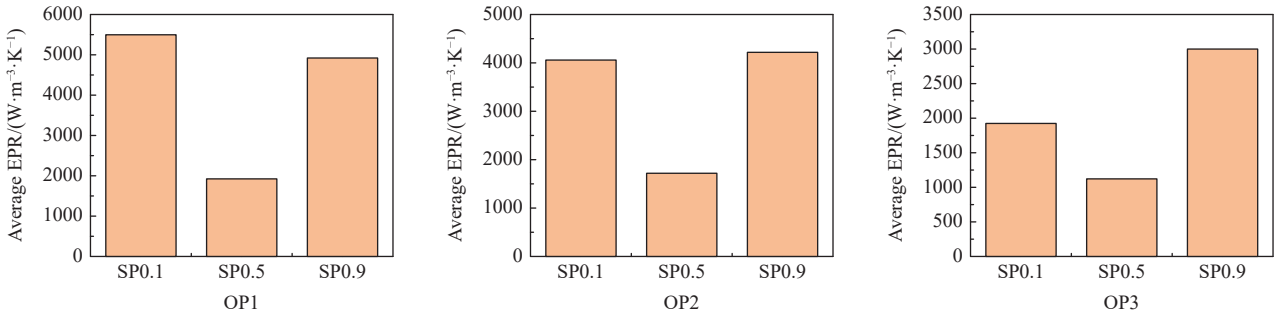

Figure 8 Comparison of average entropy production rate for different spanwise surfaces in runner channel

Due to the mismatch between the inflow direction and the rotation direction of the blade in the working condition of the reverse pump, water tends to accumulate at the tail of the blade, resulting in a large amount of energy dissipation. At the same time, under strong nonlinear turbulent motion, a small amount of water flowing out will also form vortices to block the channel, so a higher entropy production rate will also be formed at the head of the runner. The total entropy production rate distribution at both ends of the runner is higher, and lower in the middle.

It can be seen from Figure 8 that the average entropy production rate of the spanwise surface near the upper ring and the lower crown is greater than the middle spanwise surface due to the boundary layer effect. At the same time, due to water accumulation in the reverse pump condition, the average entropy production rate of the Sp0.9 surface is also significantly higher than the Sp0.1 surface.

6 Analysis of vortex rope and entropy production rate of draft tube in S-shaped region

6.1 Vortex rope in draft tube

Under runaway conditions and turbine brake conditions, the vortex at the runner outlet causes vortex rope in the center of the draft tube. Under reverse pump conditions, because the water flow accumulates at the tail of the blades, it is easy to generate backflow, which may also form vortex rope. Vortex rope will not only transmit unstable signals upstream, affect the pressure pulsation of the unit, but also affect the flow stability in the draft tube, causing unit vibration. The advantages of Omega vortex analysis method have been proved above, so Omega method is still used to identify the vortex rope of draft tube in this paper. Because the vortex rope has high rotation strength, in order to better identify, Ω=0.86 is taken. According to experience, the rotating speed of the vortex rope is far less than that of the runner, so this paper analyzes the change of the vortex rope during the transient rotation of five cycles. Figure 9 shows the changes of the vortex rope within five cycles of transient rotation under the runaway condition, turbine brake condition and reverse pump condition.

It can be seen from Figure 9 that after entering the runaway condition and the turbine brake condition, the fluid circulation at the runner outlet is large, and the reverse pressure gradient is not sufficient to cause large-scale backflow at the vortex center. A columnar vortex rope is formed at the center of the draft tube, and the center of the vortex rope is basically concentric with the straight cone section. At this time, the rotational strength of the vortex rope is high, and the change of the draft tube vortex rope is not significant as the runner rotates.

The draft tube is the inlet of the water flow under the working condition of the reverse pump, but because the rotation direction of the runner is still the working direction of the hydraulic turbine, the water flow accumulates and returns at the tail of the blade, while also having a high circulation. Therefore, vortex rope may also appear in the draft tube under this working condition. At the same time, due to the extremely unstable flow in the unit during the reverse pump working condition, the vortex rope are prone to fracture and form scattered vortices, impeding the fluid flow in the draft tube.

6.2 Entropy production rate distribution of draft tube

Draft tube is an important part of pump turbine. In addition to water diversion and drainage, it also plays an important role in recovering energy under the working condition of turbine. Therefore, this paper has studied the entropy production rate distribution of multiple sections of the draft tube, and Figure 10 shows the entropy production rate distribution under three working conditions.

As can be seen from Figure 10, the high entropy production rate area of draft tube under three conditions is mainly concentrated near the wall of the straight cone section, and there is also partial energy dissipation in the elbow section under the runaway and turbine brake condition. Along the flow direction, the entropy production rate of the runaway condition and turbine brake condition tends to decrease, while the entropy production rate of the reverse pump condition tends to increase. It can be found that the entropy production rate at the vortex rope is not larger, but the entropy production rate near the wall is significantly higher than that in the mainstream area because of the squeezing effect of the vortex rope on the water flow. Quantitative comparison of the average entropy production rate of the center section of the three conditions shows that the runaway condition is 19.46 W/m³·K, the turbine brake condition is 15.61 W/m³·K, and the reverse pump condition is 8.73 W/m³·K, which are far smaller than the runner. This is even more proof that the runner is the core location of the energy dissipation.

7 Conclusions

The aim of this paper was to analyze the vortex and energy dissipation in the S-shaped region of the pump turbine with Omega vortex analysis method and entropy production theory. The following conclusions are drawn.

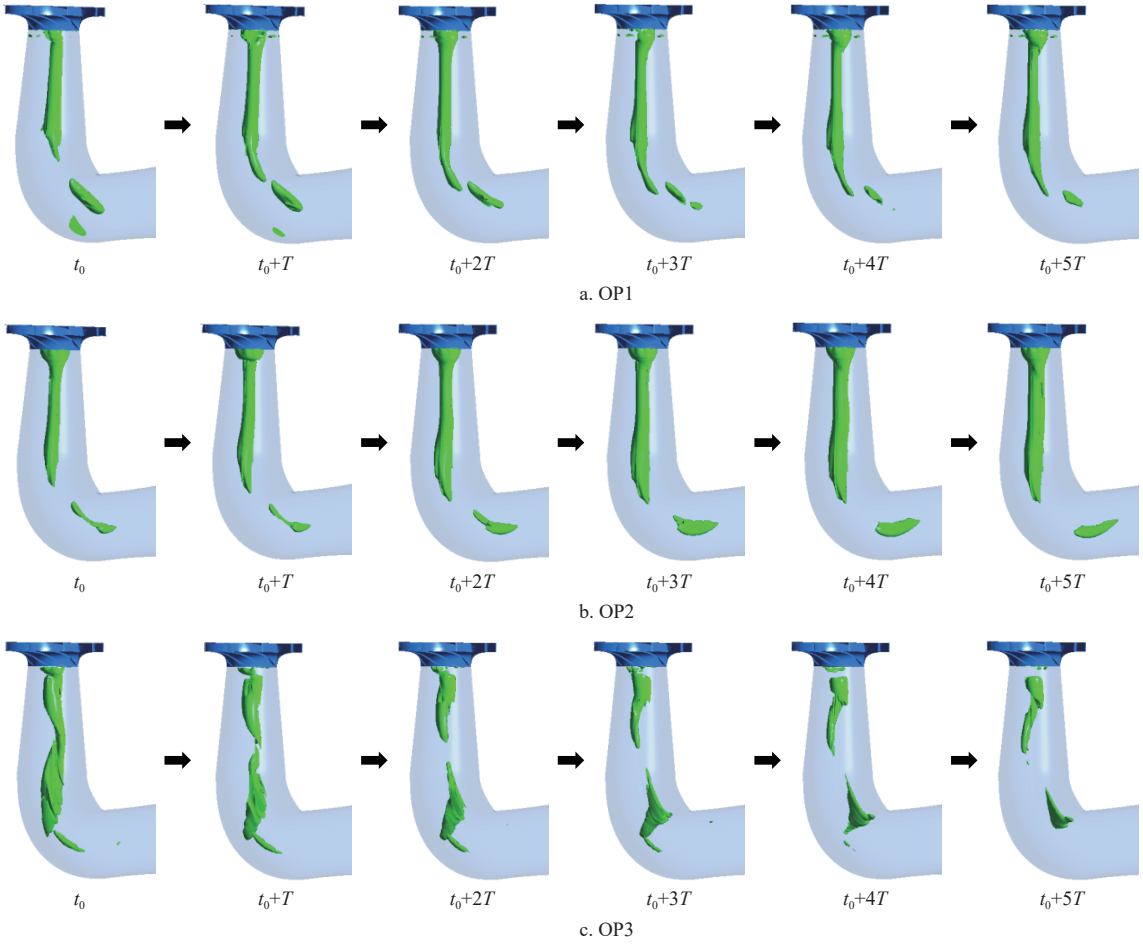

Figure 9 Change of vortex rope in draft tube

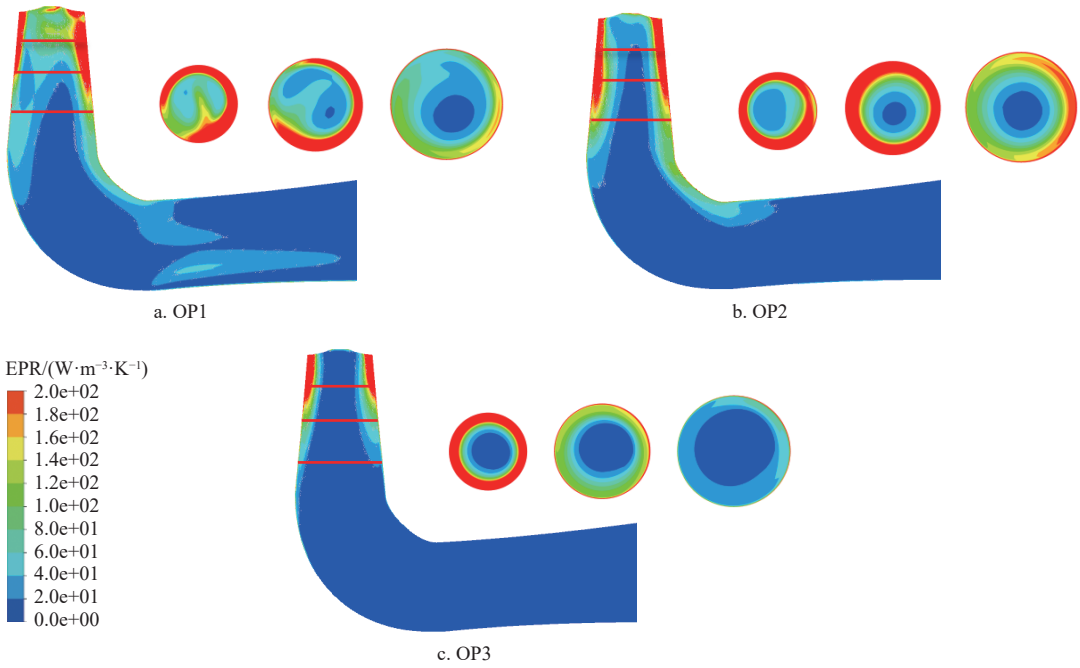

Figure 10 Entropy production rate in draft tube

1) The combination of DDES model and Omega vortex analysis method can more accurately capture the vortex evolution law at the runner in S-shaped region. The runaway condition gradually forms circulation in the vaneless space to block the channel; Under the turbine brake condition, vortices develop towards the pressure surface of the blade, causing the flow separation at the blade; Under the reverse pump condition, each channel is blocked by small-scale vortex, which makes it difficult for the water to flow into the volute and discharge smoothly, and the vorticity is larger than the other two working conditions as a whole.

2) The high entropy production rate area under runaway condition is mainly the pressure surface at the blade head of Sp0.1

surface. Under the turbine brake condition, the entropy production rate at the runner channel inlet increases significantly. The entropy production rate of the reverse pump condition runner area shows the distribution of high on both sides and low in the middle, while in the Sp0.9 surface of the blade tail the incoming impact and water flow accumulation caused a lot of energy dissipation.

3) The vortex rope of the draft tube under runaway condition and turbine brake condition is columnar, and its rotational strength is very high, squeezing the flow space of the fluid. Under the reverse pump condition, vortex rope may also be formed due to backflow, and the vortex rope may easily break into scattered vortices, resulting in chaos in the internal flow of the draft tube.

4) The entropy production rate near the wall of the straight cone section of the draft tube is high due to the squeezing effect of the vortex rope on the water flow under the three working conditions. The energy dissipation at the vortex rope is not significant. And the overall energy dissipation in the draft tube is much smaller than that in the runner region, which further proves that the runner is the core location of the energy loss of the pump turbine.

Acknowledgements

The authors acknowledge that this work was financially supported by the National Natural Science Foundation of China (Grant No. 52079118) and Sichuan Provincial Department of Science and Technology Project (Grant No. 2023YFQ0021).

Nomenclature

Symbols	Description
ω	Vorticity, s^{-1}
R	Vortical vorticity, s^{-1}
S	Non rotating vorticity, s^{-1}
Ω	Vortical vorticity/Overall vorticity
B	Antisymmetric tensor
A	Symmetric tensor
ε	Positive number
$\dot{S}_D^{\cdots}$	Entropy production rate, $W \cdot m^{-3} \cdot K^{-1}$
$\dot{Q}$	Energy dissipation rate
$\dot{S}_{\tilde{D}}^{\cdots}$	Entropy production rate due to pulsating velocity
$\dot{S}_{\bar{D}}^{\cdots}$	Entropy production rate due to the time-averaged velocity
μ_{eff}	Fluid effective dynamic viscosit, Pa·s
μ	Dynamic viscosity, Pa·s
μ_t	Turbulent power viscosity, Pa·s
ω	Turbulent vortex viscous frequency, s^{-1}
k	Turbulent kinetic energy, m^2/s^2

[References]

[1] Peng C D. Contribute to the Realization of the Goal of "Carbon peak and carbon neutrality" speed up the development of pumped storage power plants. Hydropower and Pumped Storage, 2021; 7(6): 4–6.

[2] Zeng W, Yang J D, Guo W C. Runaway instability of pump-turbines in s-shaped regions considering water compressibility. Journal of Fluids Engineering, 2015; 137(5): 051401.

[3] Adu D, Zhang J F, Fang Y J. Review on S-shape characteristics of pump turbine for hydropower generation. American Journal of Electrical Power and Energy Systems, 2017; 6(4): 43–50.

[4] Wang H J, Wang J P, Gong R Z, Shang C Y, Li D Y, Wei X Z. Investigations on pressure fluctuations in the s-shaped region of a pump-turbine. Energies, 2021; 14(20): 6683.

[5] Kinoue Y, Shiomi N, Sakaguchi M, Maeda H, Alam M M A, Okuhara S, et al. A pump system with wave powered impulse turbine. IOP Conference Series: Earth and Environmental Science, 2019; 240(5): 052009.

[6] Zhang W W, Chen Z M, Zhu B S, Zhang F. Pressure fluctuation and flow instability in S-shaped region of a reversible pump-turbine. Renewable Energy, 2020; 154: 826–840.

[7] Fu X L. Research on the load rejection transient process of pump-turbine. Harbin Institute of Technology, 2017. (in Chinese)

[8] Liu C Q, Gao Y S, Dong X R, Wang Y Q, Liu J M, Zhang Y N, et al. Third generation of vortex identification methods: Omega and Liutex/Rortex based systems. Journal of Hydrodynamics, 2019; 31(2): 205–223.

[9] Krappel T, Kuhlmann H, Kirschner O, Ruprecht A, Riedelbauch S. Validation of an IDDES-type turbulence model and application to a Francis pump turbine flow simulation in comparison with experimental results. International Journal of Heat and Fluid Flow, 2015; 55: 167–179.

[10] Mao X L, Zheng Y, Qu B, Guo C, He Z W. Analysis on the internal flow field in vaneless space and draft tube of one reversible pump turbine during load rejection under turbine mode. IOP Conference Series: Earth and Environmental Science, 2018; 163(1): 012059.

[11] Kye B, Park K, Choi H, Lee M, Kim J-H. Flow characteristics in a volute-type centrifugal pump using large eddy simulation. International Journal of Heat and Fluid Flow, 2018; 72: 52–60.

[12] Ji L, Xu L C, Peng Y J, Zhao X Y, Li Z, Tang W, Liu D M, et al. Experimental and numerical simulation study on the flow characteristics of the draft tube in francis turbine. Machines, 2022; 10(4): 230.

[13] Liu D M, Xu W L, Zhao Y Z. Experimental study of the flow field of a high head model pump turbine based on PIV technique. Journal of Hydrodynamics, 2021; 33(5): 1045–1055.

[14] Kan K, Li H Y, Chen H X, Xu H, Gong Y, Li T Y, et al. Effects of clearance and operating conditions on tip leakage vortex-induced energy loss in an axial-flow pump using entropy production method. J. Fluids Eng, 2023; 145(3): 031201.

[15] Fu X L, Li D Y, Wang H J, Zhang G H, Li Z G, Wei X Z, et al. Energy analysis in a pump-turbine during the load rejection process. Journal of Fluids Engineering, 2018; 140(10): 101107.

[16] Chen Q F. Entropy production rate analysis in S zone for a pump-turbine. Master dissertation. Beijing: Tsinghua University, 2018; 107p. (in Chinese)

[17] Li Z G, Cheng C, Yan S N, Peng S Y, Ma B. Theoretical analysis of entropy generation at the blade interface of a tubular turbine under cooperative conditions. Frontiers in Energy Research, 2021; 9: 788416.

[18] Liu C Q. Liutex-third generation of vortex definition and identification methods. Acta Aerodynamica Sinica. 2020; 38(3): 413–431, 478. (in Chinese)

[19] Li Y B, Wang Z K, Fan Z J. Numerical evaluation of unsteady flow in a centrifugal pump by omega vortex identification method. Journal of Engineering Thermophysics, 2021; 42(12): 3187–3194.

[20] Li D Y. Investigation on flow mechanism and transient characteristics in hump region of a pump-turbine. Harbin Institute of Technology, 2017. (in Chinese)

[21] Li W X, Li Z G, Zhao Q, Yan S N, Wang Z Y, Peng S Y. Influence of the solution pH on the design of a hydro-mechanical magneto-hydraulic sealing device. Engineering Failure Analysis, 2022; 135: 106091.

[22] Li W X, Li Z G, Han W, Li Y B, Yan S N, Zhao Q, et al. Pumping-velocity variation mechanisms of a ferrofluid micropump and structural optimization for reflow inhibition. Physics of Fluids, 2023; 35(5): 052005.

[23] Spalart P R, Jou W H, Strelets M, Allmaras S R. Comments on the feasibility of LES for winds, and on a hybrid RANS/LES approach. Advances in DNS/LES, 1997.

[24] Spalart P R, Deck S, Shur M L, Squires K D, Strelets K, Travin A. A new version of detached-eddy simulation, resistant to ambiguous grid densities. Theoretical & Computational Fluid Dynamics, 2006; 20(3): 181–195.

[25] Zhang Y N, Liu K H, Xian H Z, Du X Z. A review of methods for vortex identification in hydroturbines. Renewable and Sustainable Energy Reviews, 2018; 81: 1269–1285.

[26] Li W X, Li Z G, Han W, Li Y B, Yan S N, Zhao Q, et al. Measured viscosity characteristics of Fe_3O_4 ferrofluid in magnetic and thermal fields. Physics of Fluids, 2023; 35: 012002.